Available online at www.sciencedirect.com
ScienceDirect
Agricultural and Forest Meteorology 139 (2006) 138–153
AGRICULTURAL AND FOREST METEOROLOGY
www.elsevier.com/locate/agrformet

Use of a complex air pollution model to estimate dispersal and deposition of grass stem rust urediniospores at landscape scale

W. Pfender *, R. Graw, W. Bradley, M. Carney, L. Maxwell

USDA-ARS NFSPRC and Oregon State University Department of Botany and Plant Pathology, 3450 SW Campus Way, Corvallis, OR 97331, United States

Received 18 January 2006; accepted 28 June 2006

Abstract

Dispersal and dry deposition of urediniospores of *Puccinia graminis* subsp. *graminicola* from infected perennial ryegrass was modeled with CALPUFF, a Lagrangian puff atmospheric dispersal model developed for air pollution studies. The emission rate (spores/min/m^2 field area) was back-calculated from aerial spore flux from a 6 m × 6 m source plot. Spore flux was measured by a novel approach in which the cross-section of the entire plume was sampled immediately downwind of the source. The diurnal pattern of spore release was obtained from continuous volumetric spore sampler measurements in a nearby field. Weather observations at the study site were combined with three-dimensional prognostic meteorological fields generated by the Penn State Mesoscale Meteorological Model (MM5) using CALMET to run CALPUFF. The settling velocities of single and clustered spores were measured in the laboratory. Deposition fields and mass balances from the 6 m × 6 m plots were modeled by using observations from four dates in June 2005. A deposition level of 10 spores/m^2 was estimated to reach 1.8–2.1 km downwind of the plot on different days. For three of the dates CALPUFF estimated few or no spores remaining airborne as long as an hour after release above the canopy. Modeling of spore dispersal from 5- or 50-ha fields of rust-infested perennial ryegrass indicated deposition of 10 spores/m^2 at a distance of 2.1–5.9 km from the field, depending on weather and source strength (size of field and severity of rust disease), and deposition of 0.01 spores/m^2 was indicated to extend more than 12 km from a heavily infested 50-ha field for one of the days. In this scenario 10^{14} spores were released from the field in 24 h, 18 million remained airborne more than an hour and 400,000 reach the air aloft. Simulation of spore dispersal by a small dust devil showed 12.5% of the spore biomass advected horizontally beyond 200 km in the air aloft.

Keywords: Spore dispersal; Dry deposition; *Puccinia graminis*; Spore emission rate; CALPUFF

1. Introduction

Transport of air-dispersed spores of plant pathogenic fungi occurs at several epidemiologically important scales, from within-field focus expansion to transcontinental movement. In understanding and managing plant disease epidemics regionally, field-to-field movement of plant pathogen spores can be particularly important. Knowledge of the relative epidemiological importance of inoculum blown into a field from another field, as compared with local (within-field) inoculum, can guide predictions of disease development useful in management (Aylor, 1999). For this reason, estimating spore movement over a range of tenths to tens of kilometers from a source field would be useful.

The agricultural landscape in the grass seed production region of western Oregon presents conditions where spore dispersal over these short- to mid-range distances

* Corresponding author.
E-mail address: pfenderw@onid.orst.edu (W. Pfender).

0168-1923/$ – see front matter
doi:10.1016/j.agrformet.2006.06.007

may be particularly influential. Stem rust, caused by *Puccinia graminis* subsp. *graminicola*, is the most damaging disease of perennial ryegrass and tall fescue seed crops in the area, and its wind-blown urediniospores can travel over a patchwork landscape of grass seed fields. The Willamette Valley, approximately 200 km north to south and 60 km east to west, has approximately 9000 grass seed fields including over 4000 each of perennial ryegrass and tall fescue fields. Individual fields of perennial ryegrass range in size from 0.5 to 140 ha; the 10th and 90th percentile field sizes are 4 and 50 ha. In Linn County, the Oregon County with the most ryegrass acreage, the nearest-neighbor distance between perennial ryegrass fields (edge of source field to center of target field) ranges from 0.1 to 3.9 km, has a mean of 0.4 km, and 95th percentile of 1.3 km (G. Mueller-Warrant, personal communication).

There is a large literature concerning aerial transport of plant pathogen spores. Aylor (1986) describes five constituent processes as: spore production, spore escape from the crop canopy, transport and dilution of the spore cloud, spore mortality and depletion during transport, and deposition. Quantification and modeling of spore escape from the canopy is difficult and complex, and has received much attention (Aylor and Ferrandino, 1985; Aylor and Flesch, 2001; Aylor and Taylor, 1983; Aylor et al., 2001; Legg and Powell, 1979). Factors determining the escape fraction (proportion of spores that escape to the air above the canopy) include the vertical position of the source spores in the canopy and the ratio of spore settling velocity to ambient turbulence (Aylor, 1999). Spores of rust fungi commonly are dispersed as a mixture of single spores and spore clusters, with settling velocity dependent upon cluster size (Ferrandino and Aylor, 1984, 1987). Mechanism of spore release (active versus passive) and other biological aspects particular to each pathogen also mediate the influence of weather conditions on spore escape. Once escaped into the air above the canopy, initial movement of the spores in the current downwind direction can be well described within the first tens of kilometers as a Gaussian plume (Spijkerboer et al., 2002) or up to a distance of 200 km as a series of Gaussian puffs. Aylor (1999) provides equations to model this movement over the range from hundreds of meters to tens of kilometers. Long-range (hundreds of kilometers) movement is generally modeled by trajectory analysis (Davis, 1987), using Lagrangian particle models such as HY-SPLIT (Isard et al., 2005). During movement, the concentration of viable spores in the air is subject to depletion through wet and dry deposition to the ground as well as mortality. Solar radiation is the primary hazard factor for many spore types (Aylor, 1989), but stem rust spores are relatively resistant to solar damage (Maddison and Manners, 1972), especially over short durations (a day or less). Deposition on the surface of susceptible crop tissue is the final step in the successful journey of pathogen spores. This process has also been studied, particularly the quantification of deposition near (i.e., within 10 m of) the source (Aylor, 1987; Aylor et al., 1981; McCartney and Bainbridge, 1984; Roelfs and Martell, 1984).

Research on spore dispersal of *P. graminis* f. sp. *tritici*, a pathogen of wheat, shows that only 2% of the urediniospores released within the crop escape above the canopy (Roelfs and Martell, 1984), and that only 3% of those above the canopy are still airborne at a horizontal distance of 100 m (Roelfs, 1972). Nonetheless, urediniospores of this fungus have been trapped from the air at high altitudes (Stakman and Harrar, 1957).

In this paper we address the potential for movement of grass stem rust (*P. graminis* subsp. *graminicola*) urediniospores from source fields to other fields within the region, and the potential for spores to move beyond the region. Spore movement in a single direction from the source can be conveniently described by a simple plume model. However, emissions of wind-blown spores generally are carried in more than one direction from a source during the course of a day. Therefore we sought a dispersal and deposition estimation method that includes such realistic elements as variations in wind speed, direction and turbulence, due to meteorological conditions or landscape features. We used CALPUFF, an air pollution modeling system, to accomplish this goal. CALPUFF is a non-steady-state Lagrangian Gaussian puff model that has modules for gridded, time-varying, three-dimensional meteorological conditions, complex terrain effects, and wet and dry deposition (Scire et al., 2000). CALPUFF allows the use of on-site turbulence measurements of the horizontal and vertical Gaussian dispersion coefficients, but also allows for the use of similarity theory and micrometeorological variables, derived from meteorological observations and surface characteristics, to obtain these coefficients. CALPUFF utilizes a Gaussian puff formulation to calculate the concentration of a pollutant (or spores, in our application) at any given location downwind, and the deposition at user-specified locations (‘‘receptors’’) at ground level. Scire et al. (2000) describe the dispersion and deposition algorithms used in CALPUFF. The Gaussian puff

equation is shown below:

$$C = \frac{Q}{2\pi\sigma_x\sigma_y} g \exp\left[-\frac{d_a^2}{2\sigma_x^2}\right] \exp\left[-\frac{d_c^2}{2\sigma_y^2}\right]$$

$$g = \frac{2}{(2\pi)^{1/2}\sigma_z} \sum_{n=-\infty}^{\infty} \exp\left[-\frac{(H_e + 2nh)^2}{2\sigma_z^2}\right]$$

where C is the ground-level concentration (g/m^3), Q the pollutant mass (g) in the puff, σ_x the standard deviation (m) of the Gaussian distribution in the along-wind direction, σ_y the standard deviation (m) of the Gaussian distribution in the cross-wind direction, σ_z the standard deviation (m) of the Gaussian distribution in the vertical direction, d_a the distance (m) from the puff center to the receptor in the along-wind direction, d_c the distance (m) from the puff center to the receptor in the cross-wind direction, g the vertical term (m) of the Gaussian equation, H_e the effective height (m) above the ground of the puff center, h the mixed-layer height (m) and n is the extent of vertical plume spread inclusive of multiple reflections off the mixing lid and the ground.

For a horizontally symmetric puff, σ_x is equal to σ_y. The dispersion coefficients (σ_y and σ_z) are computed from on-site measured values of turbulence, σ_v and σ_w as follows:

$$\sigma_{yt} = \sigma_v t f_y\left(\frac{t}{t_{ly}}\right)$$

$$\sigma_{zt} = \sigma_w t f_z\left(\frac{t}{t_{lz}}\right)$$

σ_v is the standard deviation (m/s) of horizontal cross-wind component of the wind, σ_w the standard deviation (m/s) of vertical component of the wind, t the travel time (s) of the plume to the receptor, and t_{ly} and t_{lz} are the horizontal and vertical Lagrangian time scales (s).

The summation in the vertical term g, accounts for multiple reflections off the mixing lid and the ground. The dispersion coefficients (i.e., the standard deviation of the Gaussian distribution in the cross-wind and vertical direction) used in this study were computed from measured values of turbulence. The pollutant mass in the puff is dependent upon the release rate of the spores, the spatial extent of the release and the period of release.

Deposition flux is defined as

$$F = v_d \chi_s$$

where F is the pollutant deposition flux (g/m^2/s), v_d the deposition velocity (m/s) and χ_s is the pollutant concentration at the reference height in the surface layer (g/m^3).

We modified the reference height in CALPUFF, from 10 to 0.5 m, to better capture the concentration of spores released from canopy height near the field. The deposition velocity is based on an approach which expresses the deposition velocity as the inverse sum of ''resistances'' plus, for particulates, a gravitational settling term. Each of these terms is described in more detail in the CALPUFF User's Guide (Scire et al., 2000). The meteorological pre-processor, CALMET, uses prognostic output from the Penn State Mesoscale Meteorological Model (MM5) as an initial estimate for the wind field. The wind field is then modified to account for effects of complex terrain (e.g., blocking effects and slope flows), interpolated to 2.5 km resolution, and adjusted based upon surface and upper observations.

CALPUFF was developed for modeling movement of air pollution contaminants, including particulates, for both short and long distances. It is used extensively in regulatory permit modeling to assess pollutant concentrations, impacts on visibility, and acid deposition at distances between 50 and 200 km. It also contains the dispersion and deposition algorithms which apply at much shorter distances. The use of the ''slug'' mode is recommended for very near field applications. In the ''slug'' mode, the ''puffs'' consist of Gaussian packets of particles stretched in the along-wind direction. CALPUFF also contains wet and dry deposition algorithms which have been tested and incorporated into other dispersion models. Particle deposition is expressed in terms of atmospheric resistance through the surface layer, deposition layer resistance and gravitational settling (Slinn and Slinn, 1980; Pleim et al., 1984). Gravitational settling is a function of the particle size and density, simulated for spheres by the Stokes equation (Gregory, 1973). CALPUFF has the capability of tracking the mass balance of emitted particles for each hour into the modeling domain. For each hour, it tracks the mass emitted (which can be converted to number of particles based on mass/particle), the amount deposited, the amounts remaining in the surface mixed layer or the air above the mixed layer, and the amount advected out of the modeling domain. The versatility to address both dispersion and deposition algorithms in CALPUFF, combined with the three-dimensional meteorological and land use field, should result in more accurate model-predicted results compared with steady-state Gaussian plume models. We are not aware of its use previously in modeling plant pathogen spore dispersal.

Our objective was to model grass stem rust spore movement and deposition from a source field to target distances important in field-to-field disease spread,

using a realistic model that incorporates meteorological variability during the estimation period. In order to conduct the modeling, it was necessary to have a good estimate of emission rate of spores from the diseased crop canopy. Therefore, a supporting objective of this research was to experimentally quantify urediniospore emission rate in the field.

2. Materials and methods

2.1. Field and laboratory measurements

Urediniospore emission rates and associated weather conditions were measured in field experiments conducted at Hyslop-Schmidt Experiment Farm (44°38′N, 123°12′W), north of Corvallis, OR, USA. Perennial ryegrass (cvar Morningstar) was planted on 15 October 2004 in rows 30 cm apart in a 6 m × 6 m plot located in the middle of a 1.2 ha field. Oats (not a host for *P. graminis* subsp. *graminicola*) were planted in the remainder of the field around the ryegrass plot in October 2004. The ryegrass plants reached boot stage on 9 May 2005 and anthesis was complete by 14 June. On 14 April 2005 a 1 m diameter circular area in the center of the ryegrass plot was inoculated with urediniospores of *P. graminis* subsp. *graminicola* by lightly rubbing the plants with several previously inoculated potted plants of perennial ryegrass bearing sporulating lesions. Rust pustules were evident in the plot by the end of April. Stem rust severity was assessed periodically between 1 and 30 June. Severity was measured at 20 locations in the plot as %diseased plant area, with the aid of photographs illustrating a range of disease levels (Pfender, 2004). On each date that severity was determined, a contour map of disease levels in the plot was drawn and the area-weighted average disease severity for the plot was calculated. There was no other perennial ryegrass within approximately 1 km upwind of the test plot on sampling days. The oats surrounding the ryegrass plot were mowed during June as needed to maintain a canopy height similar to that of the ryegrass (approximately 0.5 m in June, the crop having lodged as is normal).

Emission of urediniospores from the diseased perennial ryegrass was measured with an array of samplers set in an arc downwind from the plot. The arc was located at a radius of 12 m from the center of the plot, and samplers were on poles set at intervals of 22.5° (approximately 4.5 m) along the arc (Fig. 1). There were seven sampler poles (135° of arc), and the array was centered on the downwind direction for each run. Each pole of the array held three samplers, one each at heights of 0.5, 1.5 and 2.5 m, except that each of the two outer

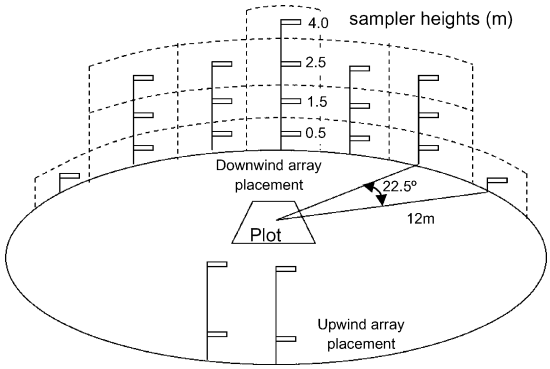

Fig. 1. Sampling array for measuring number of stem rust urediniospores in a plume emitted from a plot of diseased perennial ryegrass. Rotary impaction samplers were mounted on poles at heights of 0.5, 1.5, 2.5 and 4.0 m. The poles were set at 22.5° intervals along a 135° arc with a radius of 12 m, downwind from the center of a 6 m × 6 m plot of ryegrass infested with *Puccinia graminis* subsp. *graminicola*. Two additional poles with samplers at 0.5 and 2.5 m height were placed upwind of the plot to measure background spore concentrations. All samplers were run simultaneously during the sampling period of 30 or 60 min. To estimate total spores passing through the downwind sampling array during the sampling period, the plume cross-section was divided conceptually into rectangles (indicated here in dashed lines). Spore flux through each rectangle was derived by multiplying the spore concentration measured at the appropriate sampler by air volume moving through that rectangle. Air volume was calculated from measured or interpolated wind speed at sampler height, sampling duration and cross-sectional area of the rectangle. The spore fluxes of all rectangles were summed to produce the total flux.

flanking poles had only one sampler (0.5 m height), and the central pole of the array had four samplers (0.5, 1.5, 2.5 and 4.0 m height). Additional samplers were deployed to detect spores entering the study site from upwind. There were two upwind poles, each with two samplers (0.5 and 2.5 m height), located on the 12 m radius arc with one pole 180° from the downwind center pole and the second flanking the first depending on anticipated wind direction fluctuation. The samplers were rotary impaction devices (Aerobiology Research Laboratories, Ottawa, Ontario K2E 7Y5) that collect airborne particles on square polystyrene rods (1.6 mm × 1.6 mm × 28 mm) coated on the leading edge with silicone grease. There are two rods per sampler, located at the ends of a 9-cm long arm that spins at 2400 rpm. The greased rods are retracted (protected from contamination) until the unit is switched on and again after it is switched off. For each sampling run, the 18 samplers were turned on simultaneously and allowed to run for 30 or 60 min before being turned off.

Number of stem rust urediniospores per sampling rod was counted by microscopic examination at 200×. The background aerial spore counts for a given run, estimated by the average of all upwind samplers, was

subtracted from each downwind sampler reading before further analysis. The total number of urediniospores in the plume emanating from the plot during a defined time period (30 or 60 min) could be estimated for those runs in which the sampling array intercepted all or most of the plume, as evidenced by low or zero spore numbers on samplers at the lateral and upper margins of the array. The estimate of number of spores in the plume was made by first calculating the aerial concentration of spores measured by each sampler. Concentration was calculated as the number of spores on both rods divided by the volume of air sampled (circumference of the path of rod movement × collection rods' surface area - × number of revolutions during the sampling period). The number of spores was also corrected for the collection efficiency of the sampler, 60%. Theoretical efficiency was calculated from measured spore settling velocity and collector size and speed (Aylor, 1993) to be 86%. This value was adjusted downward to 60% based on a report (Ogden and Raynor, 1967) that pollen grains of similar size to rust spores are collected by rotary impaction samplers at about 65–70% of the theoretical efficiency. The spore flux through the sampling array was calculated by using a simple numerical integration of the observed concentrations and wind speeds, as follows. The area represented by each sampler in the array was assumed to extend half the distance to the next sampler, both horizontally and vertically (Fig. 1). The measured flux for each sampler was calculated as spore concentration (spores/m^3) × volume of air (m^3) moving past the sampler during the sample period. This air volume was calculated as the cross-sectional area of the conceptual rectangle surrounding the sampler (Fig. 1) multiplied by the wind run during the sampling period (wind speed in m/s × total seconds). Average wind speed during the sampling period for each sampler height was obtained by logarithmic interpolation (Thom, 1975) of wind speed measurements at 0.5, 2.0 and 6.7 m height. Total flux of spores through the cross-section of the spore plume was obtained by summing the fluxes from all of the samplers.

Weather data at the spore plume sampling site were collected at 5-min intervals with automated weather instrumentation (Campbell Scientific, Inc., Logan, UT, USA). Wind speed and direction were measured at 6.7 m above ground level with a rotating cup anemometer and wind vane mounted on a tower. Wind speed was measured at 2.0 and 0.5 m height also. Air temperature was measured at 6.5, 1.5 and 0.5 m height. Sensors for rainfall, total solar radiation and relative humidity were placed at 4.6, 3.9 and 1.5 m, respectively. Measurements for computing turbulence parameters (standard deviation of the vertical and horizontal wind speed) were obtained with a sonic anemometer (model CSAT3, Campbell Scientific Instruments, Logan, UT, USA) mounted at 1.7 m above ground level and facing into the wind. The sonic anemometer was operated at 1 Hz, and was located in the oats approximately 40 m away from the ryegrass plot, 45–90° from the downwind direction.

Additional data concerning diurnal spore release pattern and frequency distribution of spore clustering were obtained with a Burkard 7-day recording suction sampler (2-h resolution) operating at a height of 0.75 m. It was not desirable to place the suction sampler in the 6 m × 6 m plot where the plume was sampled, because of the effect such a large object would have on turbulence (and thus on the spore release and dispersal we were measuring). Therefore the sampler was placed in a field of rusted perennial ryegrass approximately 1 km from the plume sampling site. Counts of stem rust spores from this sampler provided a temporal profile of spore release that could be expressed as percentage of total daily release in each 2-h time increment. This diurnal pattern for each day was taken to represent the diurnal pattern at the plume sampling site on the same day. Rust spores are known to be dispersed not only as single spores, but also as clusters of two or more (Ferrandino and Aylor, 1987). We determined the distribution frequency of variously sized clusters of rust spores by counting a total of 1000 dispersal units (singlets or clusters) on Burkard sampler tapes from daytime hours on randomly selected days in June. Spores that were touching one another on the tape were considered to be clustered, and heavily populated tapes (on which clustering could not be clearly distinguished from multiple singlets impacting the tape) were not used for this assessment.

Settling velocity of *P. graminis* subsp. *graminicola* urediniospores was measured by means of a settling tube similar to that described by Ferrandino and Aylor (1984). Spores released in small numbers through a small opening at the top of a 45-cm tall tube (5 cm diameter) were collected at the bottom on greased microscope slides moved at one-second intervals through a 3-mm high gap below the tube. Light directed upward through the tube from a cool, fiber optic source allowed us to observe that spores fell uniformly, without turbulence. Slides were examined microscopically for presence and cluster sizes of spores. The settling rate average and standard deviation for single spores, and those for clusters of sizes up to seven spores, were calculated based on the time required to fall the length of the settling tube. Average mass per spore was

calculated by weighing a sample of spores, then suspending them in a known volume of light oil and counting spore number per volume of suspension with the aid of a haemocytometer. Average mass per spore was computed as total weight divided by number of spores. The CALPUFF input for effective aerodynamic spore diameter was back-calculated from the spore density and our measurements of settling velocity, using the Stokes equation. Spore density was taken to be 1.0 g/cm^3 based on reports for the closely related fungus *P. graminis* subsp. *graminis* (Gregory, 1973).

2.2. Running the CALPUFF model

A 428 km × 445 km modeling domain was created for this analysis, extending from the Oregon Coast (124°W) to eastern Oregon 119°W, and from southern Oregon (43°N) to central Washington (47°N). The experimental plot was located at 60 km east and 177 km north from the southwest corner of the grid. Meteorological data were obtained and processed as follows. MM5v3.7 was run using NCEP Eta model output as initial boundary conditions, 24 vertical levels, and a nested horizontal grid resolution of 36 km (outside grid) and 12 km (inside grid). Physical options included CCM2 radiation, Reisner graupel explicity moisture scheme, Kain-Fritsch cumulus parameterization, MRF planetary boundary layer scheme and five-layer soil model. The MM5 model output was converted from Linux to ASCII platform using the CALMM5 processor. The MM5 output was then further processed with CALMET to account for terrain effects and to format the data for use by CALPUFF. In CALMET, the hourly MM5 output was modified to account for terrain effects including slope flows, blocking effects and divergence minimization. Observations from 10 surface stations, 2 upper air stations, and the on-site weather data were then used to refine the terrain-adjusted wind fields as follows. An inverse-distance squared interpolation scheme was used, which weights the observational data heavily in the vicinity of the observation station, while the terrain-adjusted wind field dominates the interpolated wind field in the regions with no observational data. Using the CALMET generated meteorological data, CALPUFF was run with a 1-h time step, for a 24-h duration for each sampling period. Because there were no precipitation events during the days we modeled, the wet deposition module of CALPUFF was not used in the runs.

CALPUFF allows for the use of either a constant or time-varying area-source emission rate. For a short-duration release, the size of the puff is determined as a function of wind speed, atmospheric turbulence and the time step used in the model. The concentration of mass within the puff approaches that of the Gaussian plume result under the appropriate steady-state conditions. We determined the area-source emission rate, which can be expressed in units of (spores/area/time), in a way that bypasses the difficulties of calculating the canopy escape fraction. We first estimated the total flux of spores through the sampling array, as described in the previous section. Using an iterative procedure, we then found an emission rate that would produce the observed mass flux at the location of the sampling array (12 m downwind of the plot center) in CALPUFF. This approach allowed us to match the simulated emission rate to the observed spore flux, leaving the quantification of spore production, escape fraction and near-source (<12 m) deposition unresolved but unneeded for these simulations. The input for hourly emission rate was varied over the 24-h simulation run by reference to the diurnal pattern of spore release obtained from the Burkard sampler for each respective day's simulation. The daily total spore flux was determined as the quotient of observed 30- or 60-min spore flux divided by proportion of daily spore total during that time interval, and emission rate for each hour was adjusted as a proportion of the total according to the Burkard sampling results. We modeled the spore population as two types of particles, single spores or multi-spore clusters, based on settling velocity. The multi-spore cluster category was assigned a single settling velocity and standard deviation, using an average of measured values for different cluster sizes (weighted by the frequency of occurrence of each cluster size among the 1000 dispersal units observed on Burkard sample tapes described earlier).

Model runs were conducted for several scenarios. In each case we obtained CALPUFF model outputs for mass balance, with compartments for spores emitted, deposited on the surface, airborne in the mixed boundary layer, airborne above the mixed layer and advected beyond the modeling domain boundary. We also obtained model output for spatially explicit deposition to the surface, and mapped the output as deposition isopleths in units of spores/m^2. To simulate concentrations and deposition within and downwind of the area source, a two-dimensional integration (cross-wind and along wind) algorithm was used. This technique avoids the errors within and near the area source that would be obtained if the total emission were assigned to a single virtual point in the center of the field. Using the two-dimensional integration technique, the size of the modeled source area is used to determine the limits of the integration. The area-source technique is described in Section 2.11 in the

CALPUFF User's Manual (Scire et al., 2000). We modeled dispersal and deposition from the 6 m × 6 m experimental plots for the days that measurements were taken, and results from four of these runs are presented. We also modeled dispersal and deposition from simulated small (5 ha) and large (50 ha) fields on two of those days, as well as dispersal and deposition of spores occurring from a "dust devil", a type of vortex thermal updraft (Sinclair, 1969) that occurs commonly in the grass seed producing region in summer.

3. Results

3.1. Physical characteristics of P. graminis subsp. graminicola urediniospores

Observations of randomly selected dispersal units of the fungus on Burkard sampler tapes from 5 days in June (≥175 dispersal units per tape) showed that 50% (647/1293) of the urediniospores occurred singly, representing 74% of the dispersal units. The other half of the spore biomass (26% of the dispersal units) occurred in clumps of two or more spores per dispersal unit. For N (number of spores in a cluster) = 2, 3, 4, 5 and >5, the respective proportions of total biomass were 21%, 9%, 7%, 4% and 9%. The respective proportions of dispersal units were 16%, 4%, 3%, 1% and 2%.

Average spore mass was determined to be 3.43 ng/urediniospore. The settling velocity (v_s) for single urediniospores averaged 1.13 cm/s (standard deviation, S.D. = 0.055). The average v_s for clusters (size 2–7) ranged from 1.36 cm/s for clusters of 2, to 2.9 cm/s for clusters of 7, with a standard deviation (among all clusters regardless of size) of 0.313. For simplicity, we decided to treat the spore population as two subpopulations, each comprising 50% of the biomass: singlet spores with $v_s = 1.13$ and S.D. = 0.055, and spore clusters with an average $v_s = 2.12$ and S.D. = 0.313. The combination of the two means ±2 of their respective standard deviations accounted for essentially the entire range of observed v_s.

3.2. Disease development in the plot

On 2 June plants in the central 7 m^2 of the plot had a disease severity of 3% (3% of plant area diseased), surrounded by concentric areas of 2% and 0.2% severity. On 8 June severity in the center of the plot was 5% and there was a gradient to 0.5% at the plot edges. In the subsequent disease assessments plants in the center of the plot became severely stressed, supporting less pathogen sporulation, so that maximum disease levels occurred in a ring that expanded outward. The weighted mean rust severity for the plot on 3, 8, 14, 15 and 21 June was 1.5%, 2.4%, 2.6%, 2.4% and 1.7%, respectively (Table 1).

3.3. Spore dispersal from the experimental plot

The data shown in Table 1 and analyzed in the following sections are from sampling runs in which the sampling array intercepted most of the plume during the sampling period, and the number of spores caught on the upwind samplers (background spore concentrations) was less than 5% of the number caught on the central downwind sampler. The results are expressed as number of spores, rather than dispersal units (singlet or clustered

Table 1
Conditions, observations and estimates for the sampling experiment on urediniospores of *Puccinia graminis* subsp. *graminicola* from a 6 m × 6 m source plot of perennial ryegrass

Date	Sampling start time	Sampling duration (min)	Vertical temperature gradient[a] (°C/m)	Wind speed at 2.5 m (m/s)	Rust disease severity[b]	Calculated spores in plume[c] (×10^6)	Modeled emission[d] (spores × 10^6)	Modeled emission rate[e] (spores/m²/min)
3 June 2005	14:30	60	−1.18	3.0	1.5	10.1	71.5	32051
8 June 2005	14:05	60	−1.27	2.9	2.4	16.0	185.3	83023
14 June 2005	10:35	30	−0.35	2.6	2.6	15.1	58.7	52599
14 June 2005	12:55	30	−0.38	2.8	2.6	16.5	64.3	57616
14 June 2005	14:15	30	−0.97	4.2	2.6	61.0	237.5	212814
15 June 2005	11:35	30	−1.19	1.9	2.4	15.9	57.6	51587
21 June 2005	12:00	30	−1.27	5.4	1.7	44.6	233.4	209136

[a] Temperature change from 0.5 to 6.5 m above ground.
[b] Area-weighted disease severity in source plot (percentage of plant area bearing rust pustules).
[c] Urediniospores passing a sampling boundary 12 m from plot center during the sampling period, calculated from samples taken by an array of 18 rotary impaction samplers.
[d] Number of spores emitted during sample period was modeled in CALPUFF by back-calculating from observed spore flux at sampling array.
[e] Emission rate per unit area of source plot, calculated from modeled total emission.

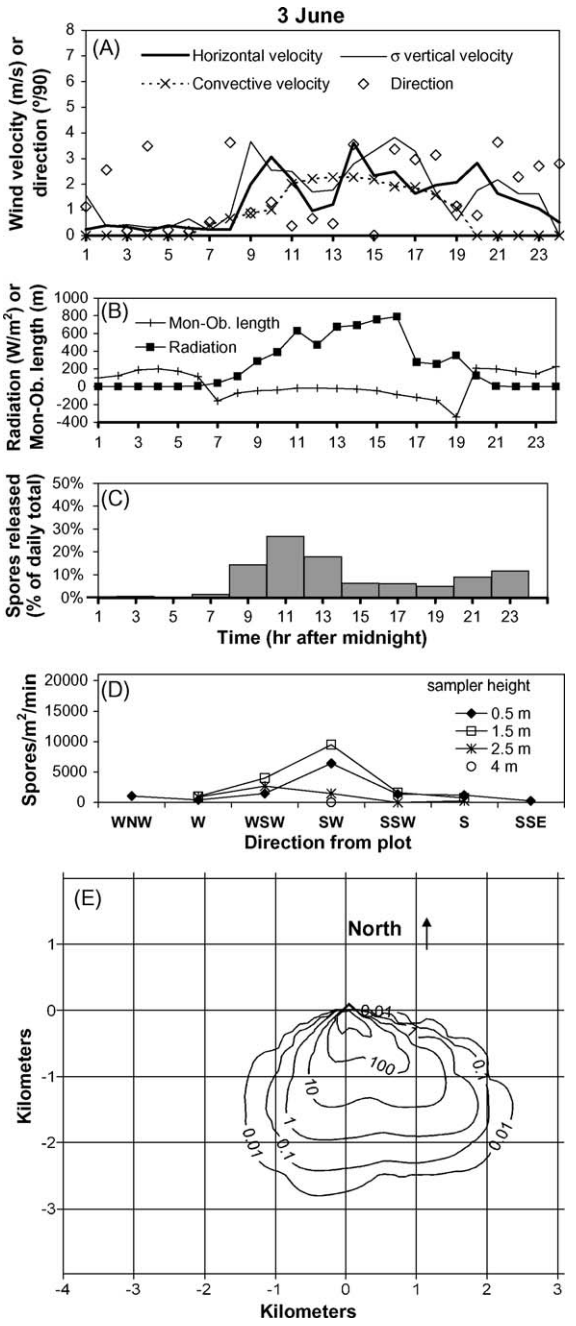

Fig. 2. Weather observations, urediniospore emission data and CALPUFF deposition model output for 3 June 2005. (A and B) Selected observed and calculated weather values at the 6 m × 6 m plot site. Horizontal wind velocity was measured at 6.7 m elevation. Variance (σ) of vertical wind velocity is multiplied by 5 for clearer presentation. Wind direction is given in degrees from north, and is divided by 90 so that 0 = North, 1 = East, 2 = South and 3 = West. Convective velocity is calculated from observations. The Monin-Obukuv (Mon-Ob.) length, also calculated by the model from observations, is positive under stable atmospheric conditions, zero under neutral conditions and negative under unstable conditions. (C) Diurnal pattern of urediniospore release, measured in 2-h increments with a volumetric suction sampler in a nearby field. Data expressed as a percent of the daily total. (D) Measured aerial urediniospore flux, during the 30- or 60-min sampling period, through a vertical plane 12 m downwind of the center of a 6 m × 6 m plot of perennial ryegrass infected with *Puccinia graminis* subsp. *graminicola*. Fluxes are shown for up to four heights at each sampler location along an arc, and background concentrations measured upwind of the plot have been subtracted. (E) Dry deposition concentrations of stem rust urediniospores emitted from the 6 m × 6 m plot during 24 h, as estimated by CALPUFF. Isopleth values are deposited spores/m^2 surface area per day.

spores); 100 spores are equivalent to approximately 70 dispersal units.

The weather data from 3 June 2005 (Fig. 2A) show that the horizontal wind velocity and the variance of the vertical velocity increased sharply at 08:00 h, whereas the convective velocity (a calculated value) increased more slowly and remained steady from 11:00 to 17:00 h. The wind was from the northeast and northwest during most of the daylight hours (Fig. 2A). Solar radiation peaked at 16:00 h, followed by a steep decrease due to cloud cover (Fig. 2B). The Monin-Obukuv length (a calculated value which is positive for stable atmospheric conditions and negative for unstable conditions) indicates instability at 07:00 and 19:00 h, and neutral conditions during most of the day (Fig. 2B). Data from the Burkard sampler in a nearby field of rusted perennial ryegrass on the same day (Fig. 2C) showed that peak spore release, 30% of the 24-h total, occurred between 10:00 and 12:00 h. Data from the sampling array 12 m downwind of the experimental plot (Fig. 2D) indicate that nearly the entire plume cross-section was sampled during the 60-min period (14:30–15:30 h) that the rotary impaction samplers were operated on that day. The flux of spores through the plane represented by the array was greatest at 1.5 m above the canopy in the center of the plume, decreasing to nondetectable at 4 m height in the plume center, and to low or nondetectable levels at the edges of the sampling array (Fig. 2D). The total flux through the sampling array was estimated from these data to be 10.1×10^6 spores during the hour (Table 1), and CALPUFF modeled this flux at 12 m from the plot with an emission rate of 32,051 spores per min per m^2 of plot area, or total release of 71.5×10^6 spores from the plot during 60 min. Because 6% of the day's total spore release occurred in a 2-h period between 14:00 and 16:00 h (Fig. 2C), our estimate of the total day spore flux from the plume source plot assumed that 71.5×10^6 spores represented 3% of the day's total (one half of the 2-h flux). Spore release during each remaining hour of the day was assigned similarly, by reference to the observed diurnal distribution in the

nearby field (Fig. 2C), to calculate emission rate inputs to CALPUFF. Results of the CALPUFF deposition modeling are shown in Fig. 2E. The illustrated 24-h deposition isopleths sum the two subpopulations (singlet spores and clusters). The model shows deposition of 10 spores/m^2 up to 1.9 km distance from the source plot, and 0.01 spore/m^2 at a maximum distance of 2.9 km. The deposition pattern reveals the influence of wind direction. The hourly mass balance calculations from the model (not shown) indicate that each hour's emission of spores was deposited within the hour, with virtually no spores persisting in the mixed layer after the hour. Under the modeled conditions, and the 1-h resolution, there was no difference between the singlet and clustered spore subpopulations with respect to deposition time. Deposition isopleths (i.e., distance of dispersal) for the two subpopulations (not shown) also were similar in location near the source plot, but at greater distances the deposition isopleths reached farther for singlets than for clusters.

The 8 June spore release was more concentrated at midday (Fig. 3C), compared to the pattern on 3 June. The sampling array was not centered on the plume (Fig. 3D), but intercepted the predominant portion of it, during the sampling period from 14:00 to 15:00 h. The estimated flux through the array was approximately 1.6 times as much as that on 3 June (Table 1). Wind speeds were somewhat higher (Fig. 3A), and midday solar radiation more intense (Fig. 3B), than on 3 June. The wind, initially from the north and east, shifted direction to southwest and south late in the afternoon (Fig. 3A). Deposition isopleths (Fig. 3E) extending to the southwest, i.e., the wind vector during the majority of the spore release, are similar in extent to those on 3 June (1.8 and 3.0 km for deposition of 10 and 0.01 spore/m^2, respectively). However changes in wind direction during the day caused the modeled deposition pattern to extend over a greater total area, with deposition of 0.01 spore/m^2 also reaching 1.7 km northwest and 2.5 km northeast of the source plot. The mass balance output from the model shows none of the clustered spores persisting in the mixed boundary layer beyond the hour of release. However, there is a small number of singlet spores (450 spores, 0.02% of those released between 02:00 and 03:00 h, and 2×10^{-5}% of the day's total) modeled to reach the mixed layer, and 35 spores remain in the mixed layer for 5 h before being deposited.

The 14 June spore flux through the sampling array, measured between 14:15 and 14:45 h, was six times as great as that in the 60-min 3 June sample (Table 1; Fig. 4D). Spore emission peaked between 14:00 and

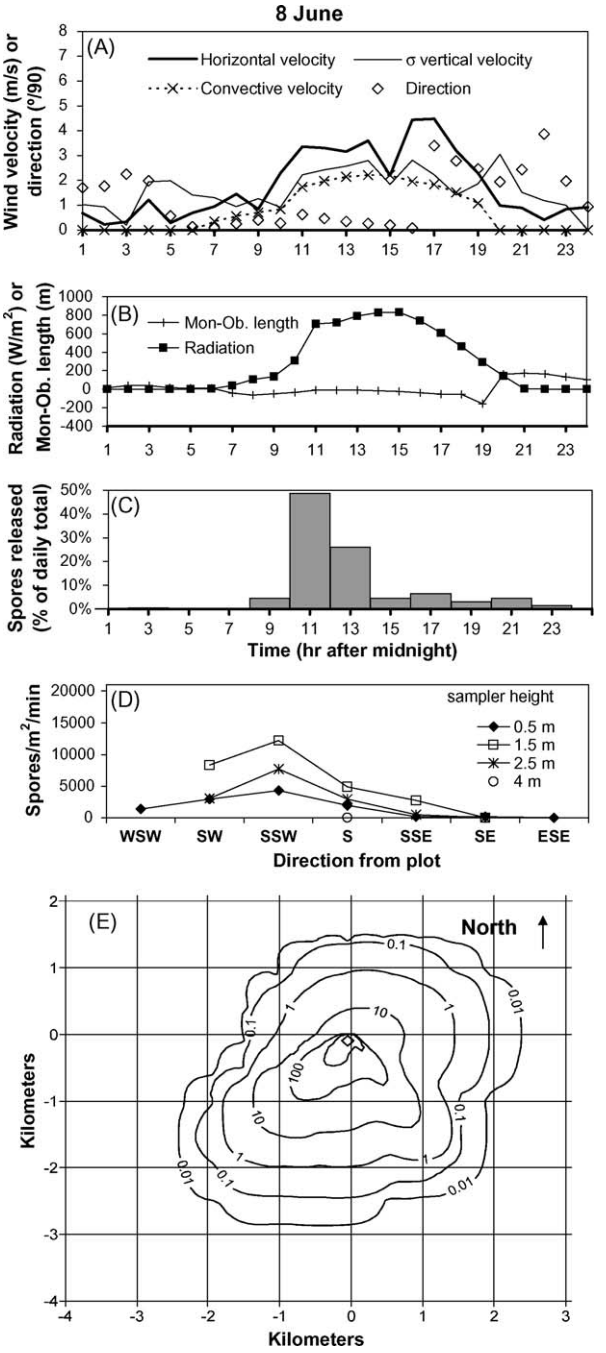

Fig. 3. Weather observations, urediniospore emission data and CALPUFF deposition model output for 8 June 2005 (see Fig. 2 caption for details).

16:00 h (Fig. 4C). Cloudiness kept the solar radiation relatively low from late morning to early afternoon (Fig. 4B). Winds were from the east briefly early and late in the day, but were predominantly from the west (Fig. 4A). The modeled resultant spore deposition (Fig. 4E) was mostly to the east, with the 10 spores/m^2

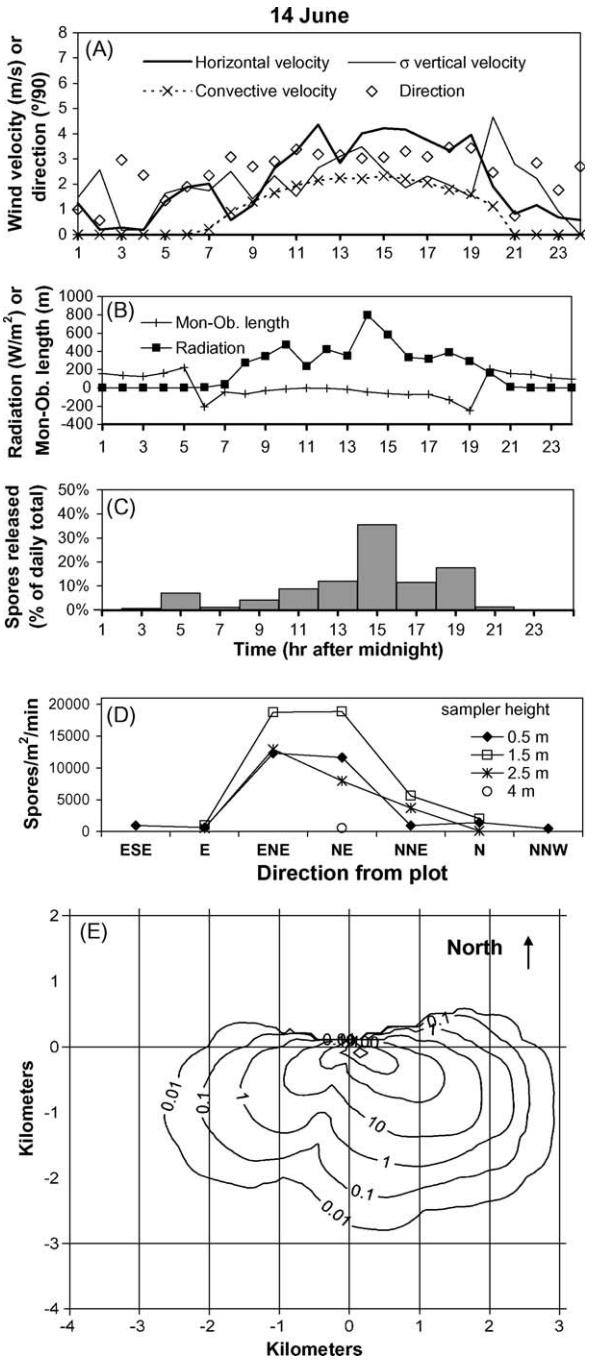

Fig. 4. Weather observations, urediniospore emission data and CALPUFF deposition model output for 14 June 2005 (see Fig. 2 caption for details).

isopleth extending 2.1 km to the southeast but only 1.1 km to the southwest. The isopleth of 0.01 deposition rate, however, was more evenly spread, reaching 3.1 and 3.2 km to the southwest and southeast, respectively. The model's mass balance output shows all spores being deposited within an hour of their release, none remaining suspended in the mixed layer beyond an hour nor reaching aloft.

Over half of the 15 June spore release occurred before noon (Fig. 5C). Spore flux through the sampling

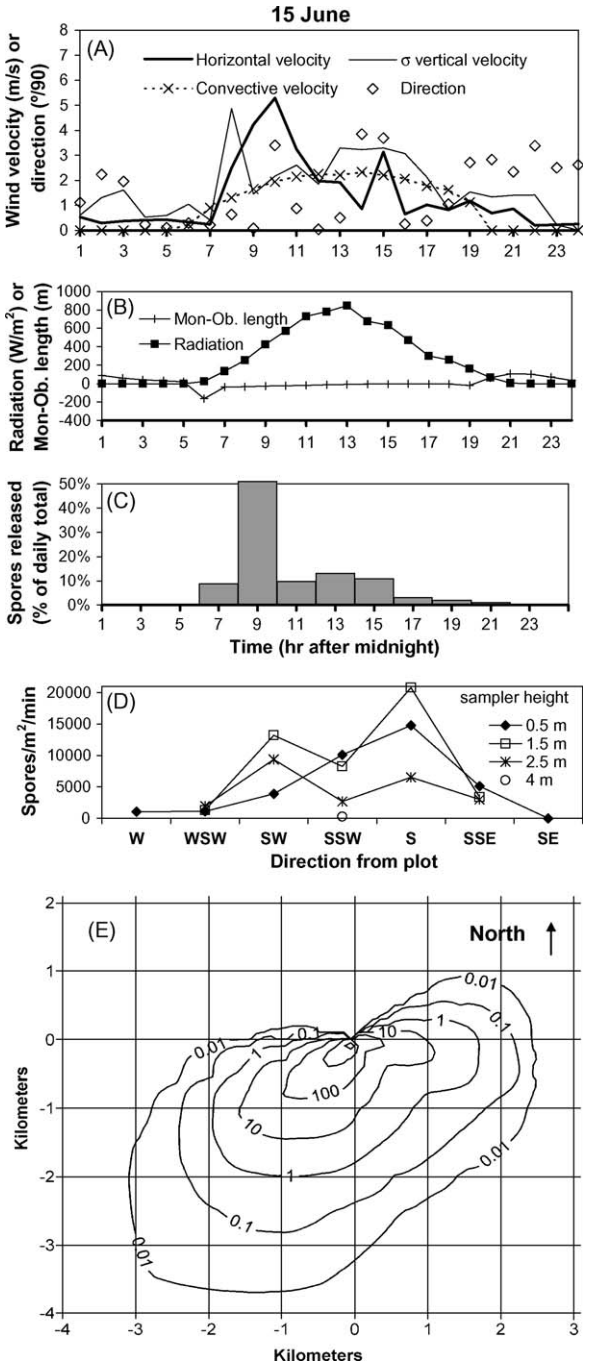

Fig. 5. Weather observations, urediniospore emission data and CALPUFF deposition model output for 15 June 2005 (see Fig. 2 caption for details).

array (Fig. 5D), measured between 11:30 and 12:00, was 1.6 times as large as that measured in 60 min on 3 June (Table 1). Solar radiation was uninterrupted during the day (Fig. 5B), and wind speeds at both 6.5 m (Fig. 5A) and 2.5 m height reached 5 m/s during the morning. Wind speed and the variance of the vertical wind velocity on 15 June were greater, and convective velocity increased earlier in the day, than on the other 3 days illustrated (Fig. 5A). Modeled spore deposition on 15 June spread mostly to the southwest, the 10 and 0.01 spores/m^2 isopleths reaching 1.9 and 4.1 km, respectively from the source plot (Fig. 5D). However, deposition of 0.01 spores/m^2 reached 2.6 km to the east also. In the mass balance calculated by the model, slightly more than 400 singlet spores (0.07% of those emitted during 1 h) remained in the mixed boundary layer past the hour in which they were released, and 6 of them reached the air above the mixed layer. None of the clustered spores was modeled to remain airborne past the hour of release.

Regression analysis of data in Table 1 showed a strong association between wind speed at 2.5 m height and the number of spores passing through the sampling array per unit time ($r^2 = 0.79$, 5 d.f.). Spore number was normalized to number per 1% rust disease severity before calculating the regression coefficient. Regression of the normalized modeled emission rate (spores/m^2/min/%rust) on wind speed (Fig. 6) had a higher correlation coefficient ($r^2 = 0.92$, 5 d.f.).

3.4. Modeled spore dispersal from large fields

Data obtained from the 6 m × 6 m plots, described in the previous section, were used to run model

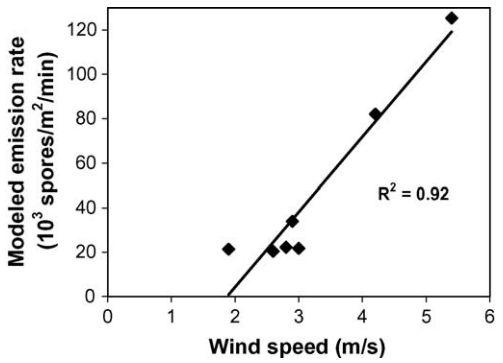

Fig. 6. Regression of modeled emission rate on wind speed for the sampling runs shown in Table 1. Emission rate is back-calculated in CALPUFF from spore flux measured at a distance of 12 m from the source, and is expressed as spores emitted per square meter plot area per minute per unit disease severity in the source plot. Wind speed was measured at 2.5 m height.

scenarios with larger sources typical of perennial ryegrass field sizes. We applied two emission rates (spores/min/m^2 of field area), representing different levels of disease severity, to each field in different model runs. Emission rates were set to 0.01 or 3 times the emission rate (ER) observed from the 6 m × 6 m plot for that date. CALPUFF accounts for proportionally larger total emission, and within-field deposition, for a large area source. The field sizes for these simulations, 5 and 50 ha, represent approximately the 10th and 90th percentile for size among perennial ryegrass fields in the Willamette Valley. We examined spore movement and deposition at the indicated emission rates for two dates, using the same weather data and diurnal emission pattern as were used for the respective 6 m × 6 m plot simulations.

The model results for two of the simulations for 15 June (smaller field with 0.01 × ER and larger field with 3 × ER) are shown in Fig. 7. For the 5-ha field, deposition levels of 10,000, 10 and 0.1 spores/m^2 reached 0.2, 2.1 and 4.3 km beyond the edge of the source field (Fig. 7A). The model run for the 50 ha field and the larger emission rate under 15 June conditions resulted in 10,000 spores/m^2 deposition as far as 2.4 km from the field, and 0.1 spores/m^2 up to 6.5 km away (Fig. 7B). The 24-h mass balance model outputs for the 50-ha field on 15 June (not shown) indicate a substantial number of spores (though a small proportion of the total) persisting for several hours in the air. For the smaller emission rate (0.01 × ER) from the 50-ha field (not shown) 60,000 of the 3×10^{11} emitted spores are in the mixed layer for several hours, and 2000 are advected out of the modeling domain, 200 km to the north, in the air above the mixed layer. For the 50-ha field with the larger emission rate (8×10^{13} spores total in 24 h), 18 million spores remain more than an hour in the mixed layer, 400,000 reach the air aloft and 350,000 are advected out of the sampling domain (>200 km from the source) at 03:00 h on 16 June.

We also selected 14 June, a day that contrasted with 15 June in weather, for modeling dispersal from 5- and 50-ha fields. Compared with 15 June, 14 June was overcast with a period of reduced solar heating before 13:00 h (Figs. 4B and 5B), a resultant smaller vertical temperature gradient (Table 1) and reduced convective velocity early in the day (Figs. 4A and 5A). Modeled total (24-h) spore emission was similar on the 2 days (1.1×10^{14} and 0.8×10^{14} on 14 June and 15 June, respectively, from 50-ha fields). Maximum distances for a range of simulated deposition levels on these 2 days are compared in Fig. 8, where only the lowest- and highest-emission scenarios are shown (i.e., 0.01 × ER

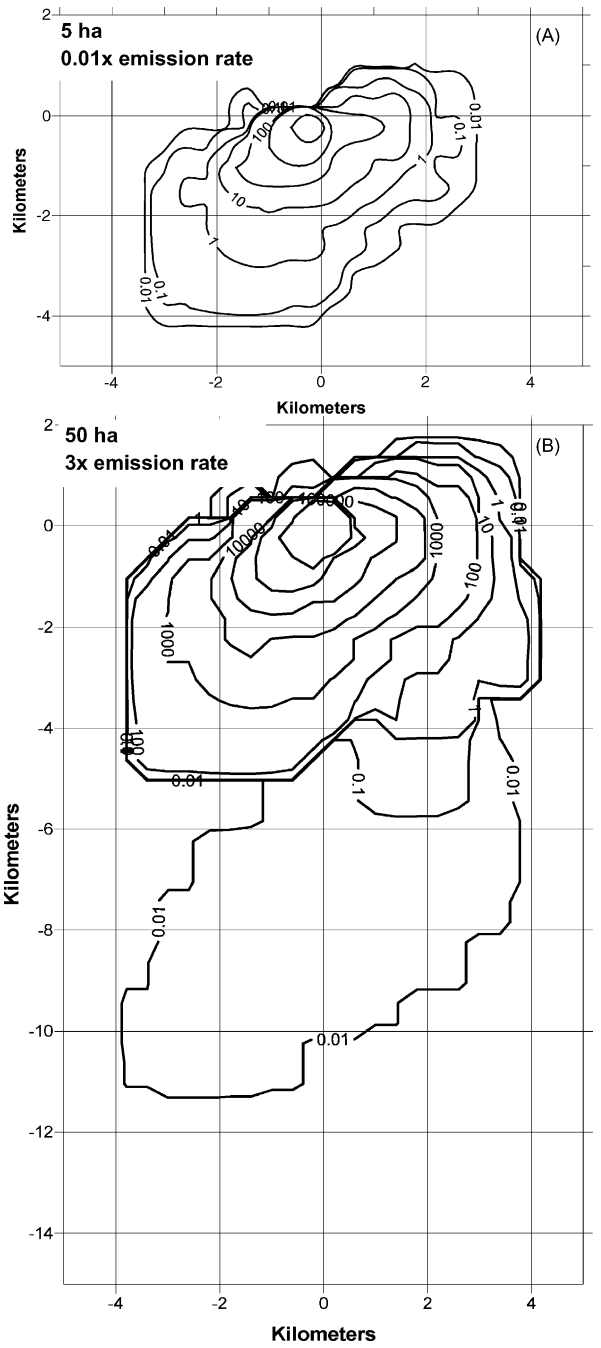

Fig. 7. CALPUFF-modeled deposition of urediniospores from simulated fields of stem rust-infested perennial ryegrass located at the same site as the 6 m × 6 m plot, using the 15 June weather data. Isopleths are spores deposited per square meter surface area. (A) Deposition of urediniospores from a 5-ha perennial ryegrass source field with an average stem rust severity of 0.02% (producing 0.01 times the emission rate that was measured from the 6 m × 6 m plot). (B) Spore deposition from a 50-ha field with an average stem rust severity of 7.2% (producing three times the emission rate measured from the 6 m × 6 m plot).

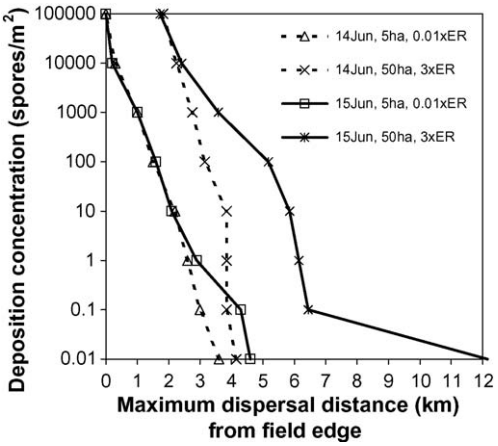

Fig. 8. Simulation results for the extent of urediniospore deposition in a 24-h period from fields of perennial ryegrass infested with stem rust. Maximum distance reached by indicated spore deposition densities from source fields with two levels of disease severity, on 2 days with differing weather. For each day, the smaller source was a 5-ha field with 0.02% rusted plant area (0.01 times the emission rate [ER] that was measured from the 6 m × 6 m plot), and the large source was a 50-ha field with 7.2% rusted plant area (three times the emission rate measured from the 6 m × 6 m plot). For each source strength, the 2 days were comparable in total spores emitted during the 24-h model period.

for 5 ha fields and 3 × ER for 50 ha fields). For the smaller source strength (smaller field and lower emission rate), the contrasting weather conditions between the 2 days affected the extent of only the lowest deposition levels, thus the deposition patterns within 3 km of the fields were similar. For the larger source strength, however, 15 June conditions resulted in greatly increased dispersal distances for deposition levels $\leq$1000 spores/m^2, in comparison with 14 June conditions, thus the deposition pattern extended 2–8 km further on the more conducive day. That is, when the spore load is large, conditions favorable to longer-distance dispersal have a greater probability of causing a measurable effect. A comparison of source strengths within either date (Fig. 8) shows that any given deposition level is displaced outward several kilometers for the larger source strength. The 24-h mass balance model outputs for the 50-ha field on 14 June (not shown) indicate only 450 of the singlet spores and none of the clusters remaining in the mixed layer past the hour of their release.

3.5. Modeling of dispersal by a dust devil

Under conditions of strong solar heating and relatively smooth terrain, an important small-scale feature of air movement is the occurrence of rotating

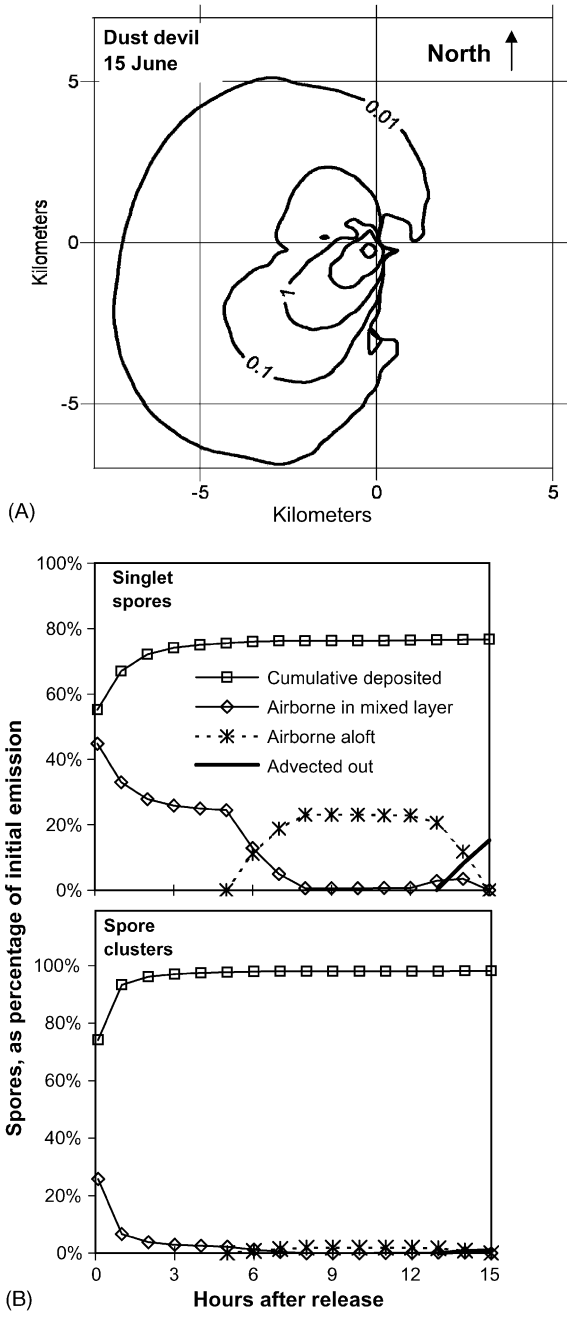

Fig. 9. CALPUFF modeling results for a simulation in which 70 million urediniospores were lifted as much as 30 m above the ground in a single event by a 6-m diameter dust devil at 15:00 h on 15 June 2005. (A) Deposition map for spores lifted in the event, in units of spores/m^2. (B) Modeled fate of spores (35 million singlets or 35 million spores in clusters), expressed as percentage of the number in the initial release. Spores lifted by the dust devil were deposited on the ground (cumulative values shown), suspended in the mixed boundary layer of the atmosphere, or suspended aloft in the air above the mixed layer. Spores remaining airborne for 15 h after the release event were advected out of the modeling domain (200 km from the source) in the absence of wet deposition.

thermal updrafts, or "dust devils" (Sinclair, 1969). Although there is variability in size and occurrence density of dust devils due to variability in conditions in the lower atmosphere, they have been observed to occur with an average frequency of three concurrent events per 10 km^2 under favorable conditions (Hess and Spillane, 1990). On hot, sunny days in grass seed fields in Oregon it is not uncommon to see several dust devils within visual range in the course of an afternoon (authors, personal observation). Although dust devils in some desert locations have been described to reach hundreds of meters in height, our personal observations have been that dust devils over cultivated grass fields in the Willamette Valley typically reach only tens of meters. For the dust devil scenario, we therefore assumed a small whirling column of air that reached 30 m above the ground surface. In the model run we assumed that a dust devil with a cross-sectional area similar to that of our 6 m × 6 m plot picked up 70 million spores (about one fifth of a typical day's total production for such an area) in a single event. For simplicity we modeled release of one third of the spores at each of three vertical levels: 10, 20 and 30 m. We chose 15 June as the modeling date, to provide conditions congruent with substantial turbulence. In so doing, we are proposing a scenario having weather conditions relatively favorable for long-distance spore movement.

The deposition map from this model run showed deposition of 1 spore/m^2 at a distance of 3.2 km from the source. Deposition of 0.1 and 0.01 spores/m^2 reached 4.8 and 7.5 km, respectively, from the source (Fig. 9A). The mass balance output from the model shows that, of the 70 million spores emitted (35 million each as singlets and clusters), most are deposited within the first hour of release (Fig. 9B). However 35% (24.5 million spores) remain in the mixed layer 2 h after the event. By 7 h after the initiation of the dust devil essentially all the spore clusters have been deposited (Fig. 9B). In contrast, approximately 25% of the singlet spores (12.5% of the spore biomass) remain suspended in or above the mixed layer for 15 h, until they are advected out of the modeling domain (200 km from the source) 16 h after the dust devil initiated the dispersal event (Fig. 9B).

4. Discussion

In this research we used a complex dispersal model, previously developed and validated for movement and deposition of air pollutants, to describe the fate of spores of a plant pathogenic fungus after release from

the crop canopy. CALPUFF provides a method for including many of the complexities of atmospheric dispersal across variable terrain. It accounts for convective and turbulent mixing, local and regional wind fields, and incorporates the physics of dry and wet deposition. Its inclusion of variable wind speeds and directions allows for a more realistic description of deposition patterns, which may radiate in multiple directions due to meandering wind, than a single-release unidirectional Gaussian description does. We also modified an important aspect of CALPUFF, setting the deposition reference height to 0.5 m (the approximate canopy height) to better capture the behavior of spores very near the ground.

Because of the difficulty in quantifying source strength for plant pathogenic fungal spores through estimates of spore standing crop and escape fraction, we applied a unique approach by measuring the total emission of spores that was airborne directly (12 m) downwind of a defined area source for a short duration. For each run of the dispersal model, this observed flux at a known boundary was used to back-calculate an emission rate to initialize the model. In this way we were assured that model results downwind of the 12 m boundary were based on an input that reflects real spore fluxes. By estimating the total emission in this way, we avoided a problem of representativeness that can arise from estimating emissions from a single sampler within a plot, viz. the unknown variation in proportion of actual emissions that are being sampled as the spore cloud shifts and changes vertical structure with varying wind speed, direction and turbulence.

We were not able to directly validate the model, estimating deposition at distances of tenths to tens of kilometers, due to the multiplicity of other sources in the area and the extreme dilution that occurs with distance as a spore cloud disperses. However, the model has previously been extensively validated for dispersal of particulates, and our use of an emission rate that matches actual observations of spore flux immediately downwind of the source should provide valid model results.

Two simplifying assumptions about urediniospore behavior were made in running the model. First, we modeled only two cluster sizes (spores per cluster), viz. singlet spores and clusters, whereas multiple cluster sizes actually occur. This simplification may result in the loss of some fine detail in modeled spore movement and deposition characteristics. But CALPUFF permits the use of a variance for a settling velocity (via a variance for effective particle diameter), and the combination of the two sizes thus allowed us to cover the frequency distribution of observed settling velocities. The settling velocity we measured for single spores is within the range of those described previously for the related fungus *P. graminis* subsp. *tritici* (Gregory, 1973). The proportion of spores occurring as singlets is similar to that reported for the bean rust fungus (Ferrandino and Aylor, 1987), although we observed the stem rust fungus to have a lower proportion of its total dispersal units as clusters. A second simplifying assumption was that the diurnal pattern of spore release at the plume study site can be inferred from the pattern measured at a site 1 km away with the Burkard sampler. This assumption affects the hourly variability in release rates used in running the CALPUFF model. To the extent that the diurnal pattern at the plume study site differs from that at the nearby site, location of deposition isopleths and the number of spores reaching the air aloft will be affected to some degree. Unless the two sites differ extremely, however, our conclusions from the model outcomes will not be substantially changed. An extreme difference is unlikely, because diurnal release pattern should be affected primarily by weather factors that would not differ greatly over 1 km distance. We decided that this source of error in the modeling effort is less problematic than the unknown but potentially important errors in measurement that would be introduced by placing a relatively large object (the Burkard recording suction sampler) in the 6 m × 6 m source plot.

Our modeling results show that the urediniospores settle quickly. Under several weather scenarios few or no spores remain airborne for as little as an hour after reaching the air above the canopy. Even under moderately turbulent conditions, the proportion of spores remaining in the mixed layer for several hours, or reaching above it, is very small. However, when the total emissions are very large (10^{14} spores released from the canopy of a 50-ha field), even a small proportion represents thousands or even millions of spores that can be distributed at least hundreds of kilometers after reaching into the atmosphere above the mixed layer. We did not model any weather scenarios with precipitation, but these spores in the upper atmosphere would presumably eventually reach the surface through wet deposition. The modeling results clearly show the importance of convective forces in the fate of these spores (which are relatively large, having a settling velocity of 1.1 cm/s) released near the ground surface. For example the relatively steep vertical temperature gradient, early increase in convective velocity and high midmorning wind speed on 15 June, combined with the morning change from stable to unstable conditions as

indicated by the Monin-Obukuv length, allowed a burst of spores to reach the air aloft. In contrast, the reduced solar radiation and resultant smaller temperature gradient on 14 June is associated with a failure of spores to remain airborne an hour after release. In this regard, an event such as a dust devil which can elevate spores tens of meters above the crop canopy is very significant in dispersal. In the dust devil scenario we modeled, 25% of the singlet spores remained airborne for 15 h after release.

The model results show significant deposition of rust urediniospores at a distance of several kilometers from a large perennial ryegrass field (Figs. 7 and 8). In interpreting these outcomes it is relevant to consider typical disease levels in source fields, and biologically significant deposition levels in target fields. The source plot for our plume study had disease levels of 1.5–2.6% during the study. This is a severe level of disease, but not uncommon. Economic losses to the ryegrass seed crop from stem rust occur at levels of approximately 0.4% and above. Very rarely, a commercial grower may experience as much as 5–10% disease severity (3 × the level in our source plot) in a field, which would produce a nearly total loss of the seed crop. Disease severities of 0.01–0.03%, only 0.01 as great as occurred in our small plot, are near the lower limit for easy visual detection in a field, and would not cause measurable damage. Therefore the range of emission rates from source fields included in the field-scale simulations covers the range from barely noticeable (0.01 × ER) to extremely damaging (3 × ER) disease levels. In calculating the impact of a given deposition level on a target field one must consider the inoculum efficiency, i.e., the percentage of spores that can successfully initiate an infection. Infection efficiency of *P. graminis* subsp. *graminicola* urediniospores has not been reported, and is a function of environmental (Pfender, 2003) and host conditions. The greatest infection efficiency for the closely related *P. graminis* subsp. *tritici* under optimal conditions is 15–25% (Rowell, 1984). Also, every 100 spores deposited in the model is equivalent to only about 70 dispersal units, due to the inclusion of spore clusters. Therefore 10% infection efficiency is a reasonable estimate for grass stem rust under field conditions, and deposition of 10 spores/m^2 in a target field would result in 1 infection/m^2. This calculation assumes all spores deposited in a target field will land on plant tissue; the assumption is appropriate because the canopy of a ryegrass field in June is dense due to lodging, and the leaf area index is >12. In the absence of other (within-field) initial inoculum, 1 infection/m^2 would be significant in starting an epidemic and producing crop damage after several pathogen generations, but would not be damaging in itself. One thousand infections per square meter, resulting from a deposition of 10,000 spores/m^2, would be near the lower threshold for direct damage, and would certainly create damaging conditions after an additional generation. For the 15 June scenario (Figs. 7 and 8) the 10 spores/m^2 isopleth extended 2.1 km from a lightly infested 5-ha field or 5.9 km from a heavily infested 50-ha field. The comparable distances for the 10,000 spores/m^2 isopleths were 0.2 and 2.4 km. On 14 June the 10-spore isopleth extended only 3.9 km from the heavily infested 50-ha source field, just 66% as far as occurred for the 15 June large-source simulation (Fig. 8). However, the 10,000-spore isopleth reached 2.4 km (the same as seen on the analogous run for 15 June). That is, the between-day weather difference had little or no effect on the maximum extent of the highest-density spore deposition, but did affect the maximum extent of the low-density deposition as modeled by CALPUFF. This was true for low- and high-disease fields, but was more marked for the high-disease fields. Given that most perennial ryegrass fields in the Willamette Valley are within 1.3 km of another such field, even a low level of disease in a source field (whether small or large) poses a risk of starting a significant epidemic in neighboring fields.

The threat of a target field receiving directly damaging inoculum levels from upwind neighboring fields is affected to some degree by source field size and disease severity. Small, lightly infested fields do not produce enough inoculum to deposit 10,000 spores/m^2 at a significant distance beyond their borders, but a large field with a similar disease severity can produce such deposits at distances of 3 km (Fig. 8). In contrast, maximum distance for deposits of this level from heavily infested source fields differs little with field size (not shown). Thus the Linn County average nearest-neighbor interfield distance of 0.4 km places more than half the fields within range of directly damaging daily inoculum from a neighboring field if the source field is sufficiently large and/or severely diseased. The preceding comments relate to the simple case of nearest-neighbor fields, whereas movement of inoculum among all fields in a region would be much more complex. Analysis of the more complex situation would allow conclusions about the relative importance of within-field and nearest-neighbor source inoculum, as compared with combined inoculum from more distant fields, in epidemic development. Regional maps of grass seed field locations and sizes for all seed-producing counties are becoming available (G. Mueller-Warrant, personal

communication), and such analyses will then be possible.

References

Aylor, D.E., 1986. A framework for examining inter-regional aerial transport of fungal spores. Agric. For. Meteorol. 38, 263–288.

Aylor, D.E., 1987. Deposition gradients of urediniospores of *Puccinia recondita* near a source. Phytopathology 77, 1442–1448.

Aylor, D.E., 1989. Aerial spore dispersal close to a focus of disease. Agric. For. Meteorol. 47, 109–122.

Aylor, D.E., 1993. Relative collection efficiency of rotorod and Burkard spore samplers for airborne *Venturia inaequalis* ascospores. Phytopathology 83, 1116–1119.

Aylor, D.E., 1999. Biophysical scaling and the passive dispersal of fungus spores: relationship to integrated pest management strategies. Agric. For. Meteorol. 97, 275–292.

Aylor, D.E., Ferrandino, F.J., 1985. Escape of urediniospores of *Uromyces phaseoli* from a bean field canopy. Phytopathology 75, 1232–1235.

Aylor, D.E., Flesch, T.K., 2001. Estimating spore release rates using a Lagrangian stochastic simulation model. J. Appl. Meteorol. 40, 1196–1208.

Aylor, D.E., Fry, W.E., Mayton, H., Andrade-Piedra, J.L., 2001. Quantifying the rate of release and escape of *Phytophthora infestans* sporangia from a potato canopy. Phytopathology 91, 1189–1196.

Aylor, D.E., McCartney, H.A., Bainbridge, A., 1981. Deposition of particles liberated in gusts of wind. J. Appl. Meteorol. 20, 1212–1221.

Aylor, D.E., Taylor, G.S., 1983. Escape of *Peronospora tabacina* spores from a field of diseased tobacco plants. Phytopathology 73, 525–529.

Davis, J.M., 1987. Modeling the long-range transport of plant pathogens in the atmosphere. Annu. Rev. Phytopathol. 25, 169–188.

Ferrandino, F.J., Aylor, D.E., 1984. Settling speed of clusters of spores. Phytopathology 74, 969–972.

Ferrandino, F.J., Aylor, D.E., 1987. Relative abundance and deposition gradients of clusters of urediniospores of *Uromyces phaseoli*. Phytopathology 77, 107–111.

Gregory, P.H., 1973. The Microbiology of the Atmosphere. Halstead Press, New York, 377 pp.

Hess, G.D., Spillane, K.T., 1990. Characteristics of dust devils in Australia. J. Appl. Meteorol. 29, 501–507.

Isard, S.A., Gage, S.H., Comtois, P., Russo, J.M., 2005. Principles of the atmospheric pathway for invasive species applied to soybean rust. Bioscience 55, 851–861.

Legg, B.J., Powell, F.A., 1979. Spore dispersal in a barley crop: a mathematical model. Agric. Meteorol. 20, 47–67.

Maddison, A.C., Manners, J.G., 1972. Sunlight and viability of cereal rust uredospores. Trans. Br. Mycol. Soc. 59, 429–443.

McCartney, H.A., Bainbridge, A., 1984. Deposition gradients near to a point source in a barley crop. Phytopath. Z. 109, 219–236.

Ogden, E.C., Raynor, G.S., 1967. A new sampler of airborne pollen: the rotoslide. J. Allergy 40, 1–11.

Pfender, W.F., 2004. Effect of autumn planting date and stand age on severity of stem rust in seed crops of perennial ryegrass. Plant Dis. 88, 1017–1020.

Pfender, W.F., 2003. Prediction of stem rust infection favorability, by means of degree hour wetness duration, for perennial ryegrass seed crops. Phytopathology 93, 467–477.

Pleim, J., Venkatram, A., Yamartino, R.J., 1984. ADOM/TADAP Model Development Program, vol. 4, The Dry Deposition Model. Ontario Ministry of the Environment, Rexdale, Ontario, Canada.

Roelfs, A.P., 1972. Gradients in horizontal dispersal of cereal rust uredospores. Phytopathology 62, 70–76.

Roelfs, A.P., Martell, L.B., 1984. Uredospore dispersal from a point source within a wheat canopy. Phytopathology 74, 1262–1267.

Rowell, J.B., 1984. Controlled infection by *Puccinia graminis* f. sp tritici under artificial conditions. In: Bushnell, W.R., Roelfs, A.P. (Eds.), The Cereal Rusts, vol. I, Origins, Specificity, Structure, and Physiology. Academic Press, New York, pp. 292–332.

Scire, J.S., Strimaitis, D.G., Yamartino, R.J., 2000. Guide for the CALPUFF Dispersion Model (Version 5.0) Earth Tech, Concord, MA.

Sinclair, P.C., 1969. General characteristics of dust devils. J. Appl. Meteorol. 8, 32–45.

Slinn, S.A., Slinn, W.G.N., 1980. Predictions for particle deposition on natural waters. Atmos. Environ. 14, 1013–1016.

Spijkerboer, H.P., Beniers, J.E., Jaspers, D., Schouten, H.J., Goudriaan, J., Rabbinge, R., van der Werf, W., 2002. Ability of the Gaussian plume model to predict and describe spore dispersal over a potato crop. Ecol. Modell. 155, 1–18.

Stakman, E.C., Harrar, J.G., 1957. Principles of Plant Pathology. Ronald Press, New York.

Thom, A.S., 1975. Momentum, mass and heat exchange of plant communities. In: Monteith, J.L. (Ed.), Vegetation and the Atmosphere, vol. 1, Principles. Academic Press, New York, pp. 57–109.